Deepwater overflow through Luzon Strait

Tangdong Qu
International Pacific Research Center, SOEST, University of Hawaii, Honolulu, Hawaii, USA

James B. Girton
Applied Physics Laboratory, University of Washington, Seattle, Washington, USA

J. A. Whitehead
Department of Physical Oceanography, Woods Hole Oceanographic Institution, Woods Hole, Massachusetts, USA

Received 1 July 2005; revised 9 August 2005; accepted 29 August 2005; published 10 January 2006.

[1] This study examines water property distributions in the deep South China Sea and adjoining Pacific Ocean using all available hydrographic data. Our analysis reveals that below about 1500 m there is a persistent baroclinic pressure gradient driving flow from the Pacific into the South China Sea through Luzon Strait. Applying hydraulic theory with assumptions of zero potential vorticity and flat bottom to the Luzon Strait yields a transport estimate of 2.5 Sv (1 Sv = 10^6 m^3 s^{-1}). Some implications of this result include: (1) a residence time of less than 30 years in the deep South China Sea, (2) a mean diapycnal diffusivity as large as 10^{-3} m^2 s^{-1}, and (3) an abyssal upwelling rate of about 3×10^{-6} m s^{-1}. These quantities are consistent with residence times based on oxygen consumption rates. The fact that all of the inflowing water must warm up before leaving the basin implies that this marginal sea contributes to the water mass transformations that drive the meridional overturning circulation in the North Pacific. Density distributions within the South China Sea basin suggest a cyclonic deep boundary current system, as might be expected for an overflow-driven abyssal circulation.

Citation: Qu, T., J. B. Girton, and J. A. Whitehead (2006), Deepwater overflow through Luzon Strait, *J. Geophys. Res.*, *111*, C01002, doi:10.1029/2005JC003139.

1. Introduction

[2] Luzon Strait is the only deep connection between the South China Sea and the Pacific, with the deepest sill at about 2400 m in the Bashi Channel (Figure 1). In the deep South China Sea, water is relatively homogenous and appears to have the same characteristics as the Pacific water at about 2000 m [*Nitani*, 1972; *Broecker et al.*, 1986; *Qu*, 2002]. This has been interpreted as evidence for the deep South China Sea ventilation by water from the Pacific passing over the Luzon Strait. Since the Pacific water is colder and of higher density, it sinks after crossing the Luzon Strait [*Wyrtki*, 1961]. To compensate this descending movement, upwelling must occur elsewhere, and thus the renewal of the South China Sea deep water is rapid compared with its Pacific counterpart [*Broecker et al.*, 1986]. While the overflow of the Pacific water through the Luzon Strait may not exert an immediate influence on the upper layer heat content, it is true that the understanding of upper layer heat content in the South China Sea relies on knowledge of the lower boundary condition, in particular with regard to the long timescale variations [e.g., *Qu et al.*, 2004].

0148-0227/06/2005JC003139$09.00

[3] A few hydrographic surveys have been able to measure the deepwater distribution in and around the Luzon Strait, confirming the existence of cold and saline Pacific water in the northern South China Sea [*Chu*, 1972; *Wang*, 1986]. On the basis of this information and combined with upwelling estimates from a one-dimensional advective-diffusive heat balance applied to the abyssal stratification of the South China Sea, *Wang* [1986] argued that about 0.7 Sv (1 Sv = 10^6 m^3 s^{-1}) of cold water must upwell from below (>1500 m) in order to establish a stable thermocline which otherwise would be gradually diminished by downward surface heat flux. This provided a quantitative, albeit indirect, transport estimate of the deepwater overflow through the Luzon Strait into the South China Sea. Such estimates, however, depend strongly on the diffusion coefficient used, in this case 10^{-3} m^2 s^{-1}. As a consequence, little further progress has been made since then in quantifying the deepwater transport using hydrographic data.

[4] The only direct measurement of the inflow of which we are aware was from a single 82-day current meter time series near the bottom of the Bashi Channel [*Liu and Liu*, 1988]. The record showed a persistent near-bottom inflow to the South China Sea with a mean speed of 0.14 m s^{-1}. Assuming a mean deep current velocity profile increasing linearly from zero at 1500 m to the maximum at 2000 m and

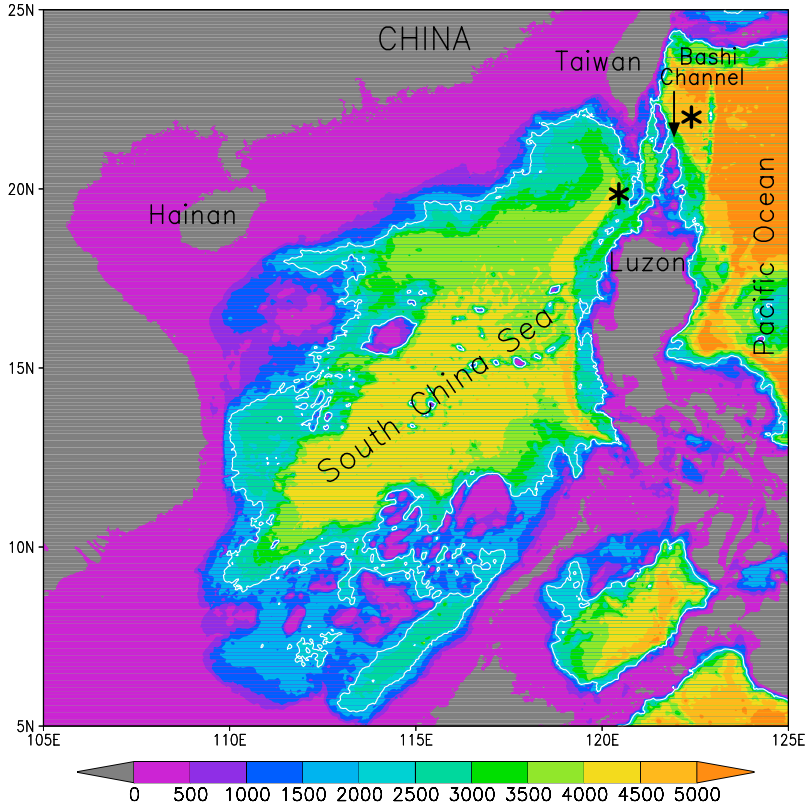

Figure 1. Bottom topography of the South China Sea [*Smith and Sandwell*, 1997]. The thick solid (white) line indicates the 2000-m isobath. Asterisks indicate the approximate locations of profiles used for Figure 7.

remaining constant to the bottom, the measurement provided a transport estimate of 1.2 Sv. Though this single record cannot quantify the transport with any given accuracy, the mean speed and direction of the deepwater overflow are consistent with earlier hydrographic observations.

[5] We wish to point out that the theory of topographic control allows a fresh look at this problem. The topographic control of fluid flowing through constrictions has been studied in a number of situations involving compressible, free surface, stratified or rotating fluid. One class of these problems describes the flow of an inviscid, rotating, reduced-gravity fluid flowing out of a narrow passage from a deep reservoir [*Whitehead et al.*, 1974]. *Whitehead* [1989] developed a methodology for applying the theory to the continuously stratified ocean, producing estimates of volume transport through a number of deep passages and straits based solely on upstream and downstream density profiles. The results indicate that rotating hydraulic control may contain appropriate dynamics for deepwater exchange.

[6] To predict the deepwater overflow through Luzon Strait using hydraulic theory requires information on density distribution in both the Pacific Ocean and the South China Sea. The most comprehensive collection of deep ocean hydrographic data is the World Ocean Atlas prepared at NOAA's National Ocean Data Center. As noted by several earlier studies [e.g., *Qu and Lindstrom*, 2004], however, this gridded atlas is not especially accurate in the western Pacific marginal seas, where the circulation is highly variable both in space and time. Under this circumstance, a more carefully-constructed climatological data set in the region is desirable.

[7] This study is intended to (1) construct a new temperature climatology in the deep South China Sea and the surrounding western North Pacific, (2) apply hydraulic theory to the Luzon Strait to estimate the transport of deepwater overflow, and (3) further examine the effect of the overflow on the deepwater circulation and property distributions in the South China Sea. The results are presented as follows. In section 2, we provide a basic background of hydraulic theory and introduce the formulas used for the volume flux estimate. In section 3, we describe the data and methods of analysis. Section 4 is devoted to a detailed description of density fields, and section 5 to the estimates of volume flux through Luzon Strait using hydraulic theory. The possible impact of the overflow on the deep South China Sea circulation is discussed in section 6, and the results are finally summarized in section 7.

2. Hydraulic Theory

[8] In hydraulic theory, one can consider a layer of water with density $\rho + \Delta\rho$ lying below a layer of motionless fluid with slightly lower density ρ. Assuming slow variation of flow in the alongstream direction, the reduced gravity shallow water momentum equations reduce to a set of

Table 1. Statistics of the Data Used for the Present Study[a]

	≥1500 m	≥2000 m	≥2500 m	≥3000 m	≥3500 m
			T/S		
Whole	1,062	409	196	148	101
SCS	553	264	92	58	33
			Oxygen		
Whole	571	167	101	85	63
SCS	211	56	25	21	15

[a]SCS is South China Sea.

ordinary differential equations describing the flow in the bottom layer. When the bottom layer in the upstream basin is infinitely deep, the zero potential vorticity assumption can be made, which further reduces the problem as follows [*Whitehead et al.*, 1974]:

$$g' \frac{\partial h}{\partial x} = fv \tag{1}$$

$$\frac{\partial v}{\partial x} = -f, \tag{2}$$

where $g' = g\Delta\rho/\rho$, f is the Coriolis parameter, g is the acceleration due to gravity, v is velocity through an ocean passage (in the y direction), and h is the height of the interface separating the two layers. Equation (1) is the geostrophic balance between the Coriolis force and the pressure gradient force at the right angle to the flow (in the x direction). Equation (2) represents the conservation of potential vorticity.

[9] Applying Bernoulli's law and maximizing volume flux using a critical control calculation [*Whitehead et al.*, 1974; *Gill*, 1977] result in the following predictions for volume flux, Q, through deep passages in the ocean,

$$Q = \frac{g' h_u^2}{2f} \qquad L > \left(\frac{2g' h_u}{f^2}\right)^{1/2} \tag{3}$$

$$Q = \left(\frac{2}{3}\right)^{3/2} L\sqrt{g'}\left[h_u - \frac{f^2 L^2}{8g'}\right]^{3/2} \qquad \text{otherwise,} \tag{4}$$

where L is width of the passage, h_u is the upstream fluid interface height above sill depth of the passage, and $R = (2g' h_u/f^2)^{1/2}$ is the Rossby radius.

[10] Formulas (3) and (4) have been used to determine volume fluxes through a number of deep passages and straits in the ocean [*Whitehead*, 1998]. They provide the greatest volume fluxes of all possible potential vorticity distributions [*Whitehead*, 2003]. These topographic control formulas are useful predictions, and provide in almost all cases a reliable upper bound of volume fluxes, with the ratio of prediction to direct measurement ranging from 1.2 to 1.5. To apply the hydraulic theory to the Luzon Strait is an important objective of the present study.

3. Data and Methods of Analysis

[11] This study uses all temperature, salinity, and dissolved oxygen concentration profiles at observed levels from the World Ocean Database 2001 for the region 5°N–25°N, 105°E–125°E, which includes part of the western Pacific. We first dropped those profiles that were flagged as "bad" or not passing the monthly, seasonal, and annual standard deviation checks, and those profiles that were shallower than 1500 m, eliminating coastal stations. Then we removed those profiles with obviously erroneous records, including those with vertical separation between two observed levels larger than 1000 m. The final data set used for this study consists of 1062 temperature/salinity profiles and 553 oxygen profiles, spanning the period from the 1920s to the beginning of the 21st century (Table 1). At 2000 m, there are 409 temperature/salinity samples in the region studied, and at 3500 m, the number drops to101, with only 33 in the South China Sea (Figure 2). The spatial distribution of oxygen profiles has essentially the same pattern as temperature/salinity, except for a lower sampling density (Table 1). See *Qu* [2002] for details.

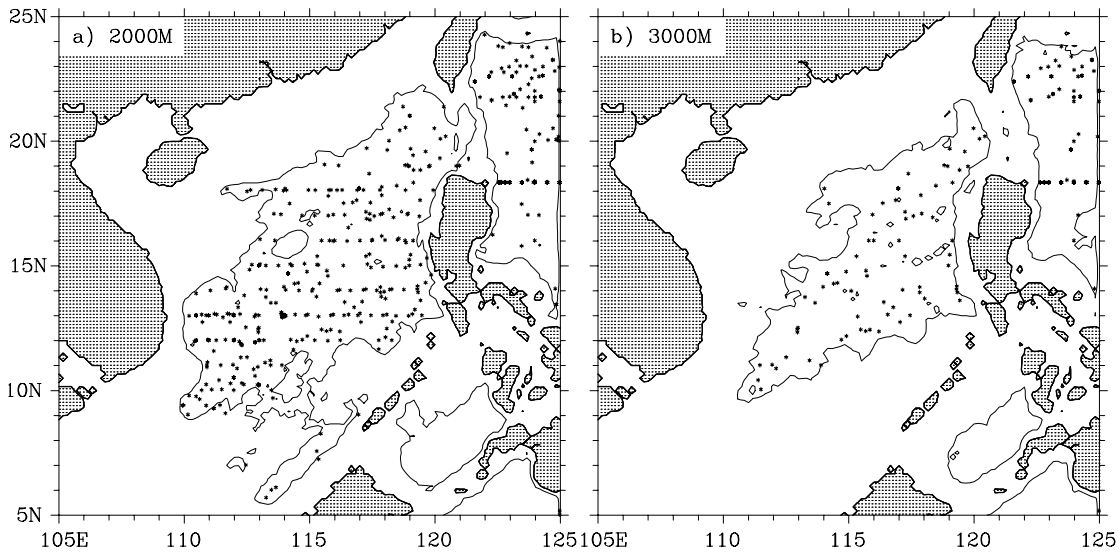

Figure 2. Geographical distributions of temperature and salinity profiles used in this study.

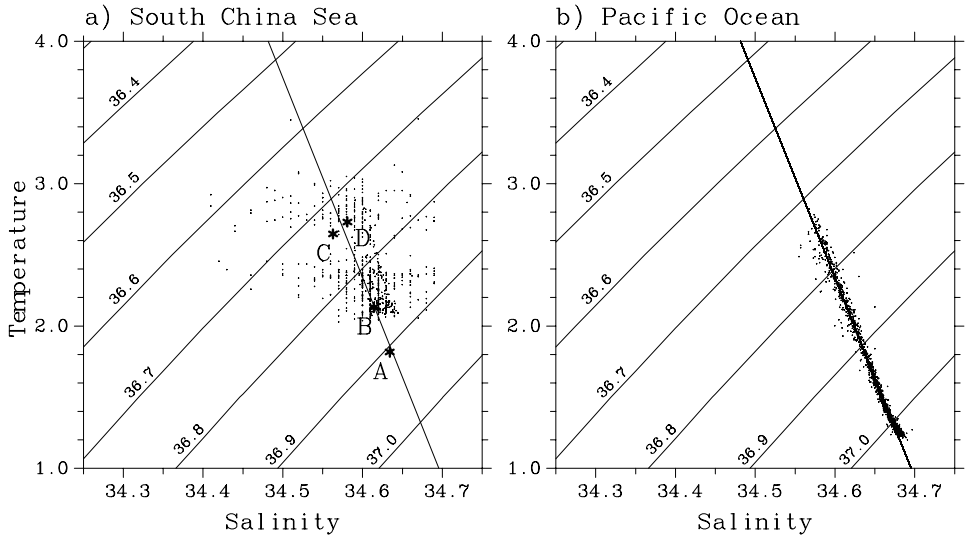

Figure 3. Relation of potential temperature versus salinity (with σ_2 contours overlain) in the deep ($\geq$1500 m) South China Sea and the Pacific. Data used consist of 255 profiles over the entire South China Sea and 101 profiles in the region (122°E–125°E, 18°N–23°N) east of the Luzon Strait. The thick line represents the linear regression of the potential temperature versus salinity relation in the Pacific. Asterisks A and B on the left panel represent water properties at sill depth (2181 m) on the Pacific and South China Sea side of Luzon Strait, respectively. Asterisks C and D are the same as A and B except at the bifurcation depth (1489 m, see text for detail).

[12] Water in the deep South China Sea is relatively homogenous [*Nitani*, 1972; *Broecker et al.*, 1986, *Qu*, 2002]. At depths $\geq$1500 m, potential density (reported as σ_2 hereinafter, where σ_2 + 1000 kg m^{-3} denotes potential density referenced to 2000 decibar) lies mostly between 36.7 and 36.8 kg m^{-3}, significantly lighter than its counterpart in the Pacific (Figure 3). In all 33 of the deep World Ocean Database profiles, potential temperature decreases with depth, and the mean value drops from 2.36°C at 2000 m to 2.11°C at 3500 m (Figure 4). Given a typical standard deviation of only about 0.03°C, this result suggests a well-stratified thermal structure in the deep South China Sea. Unfortunately, the relation of potential temperature versus salinity shows far greater salinity scatter than is reasonable for a deep isolated basin (Figure 3a). At a given potential temperature between about 2° and 3°C, the range of salinity variations can be as large as 0.3 psu.

[13] Most of the salinity data archived in the World Ocean Database were collected in or prior to the 1970s. The quality of these early observations is generally bad (Figure 4).

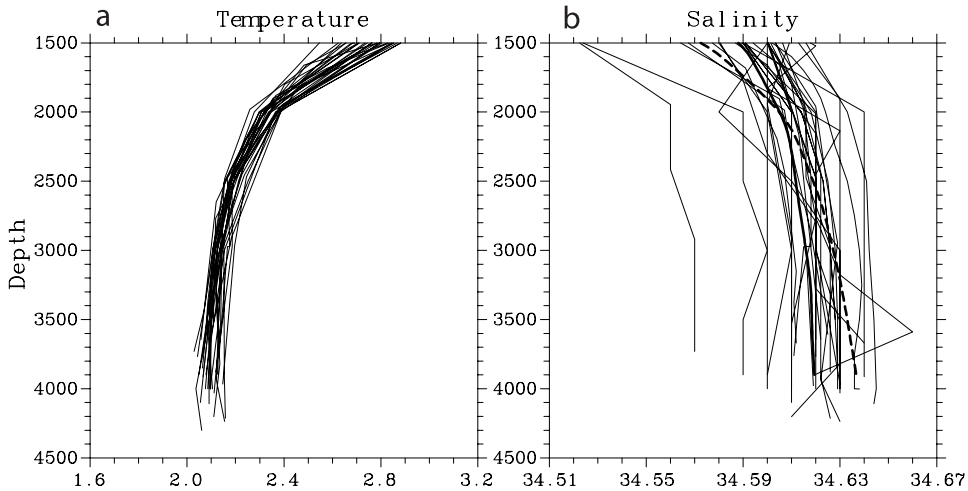

Figure 4. Vertical profiles of potential temperature (°C) and salinity (psu) of those (33) extending to 3500 m or below in the deep South China Sea. The thick solid line on Figure 4b represents the simply averaged salinity, and the thick dashed line represents the synthetic salinity from the 33 profiles.

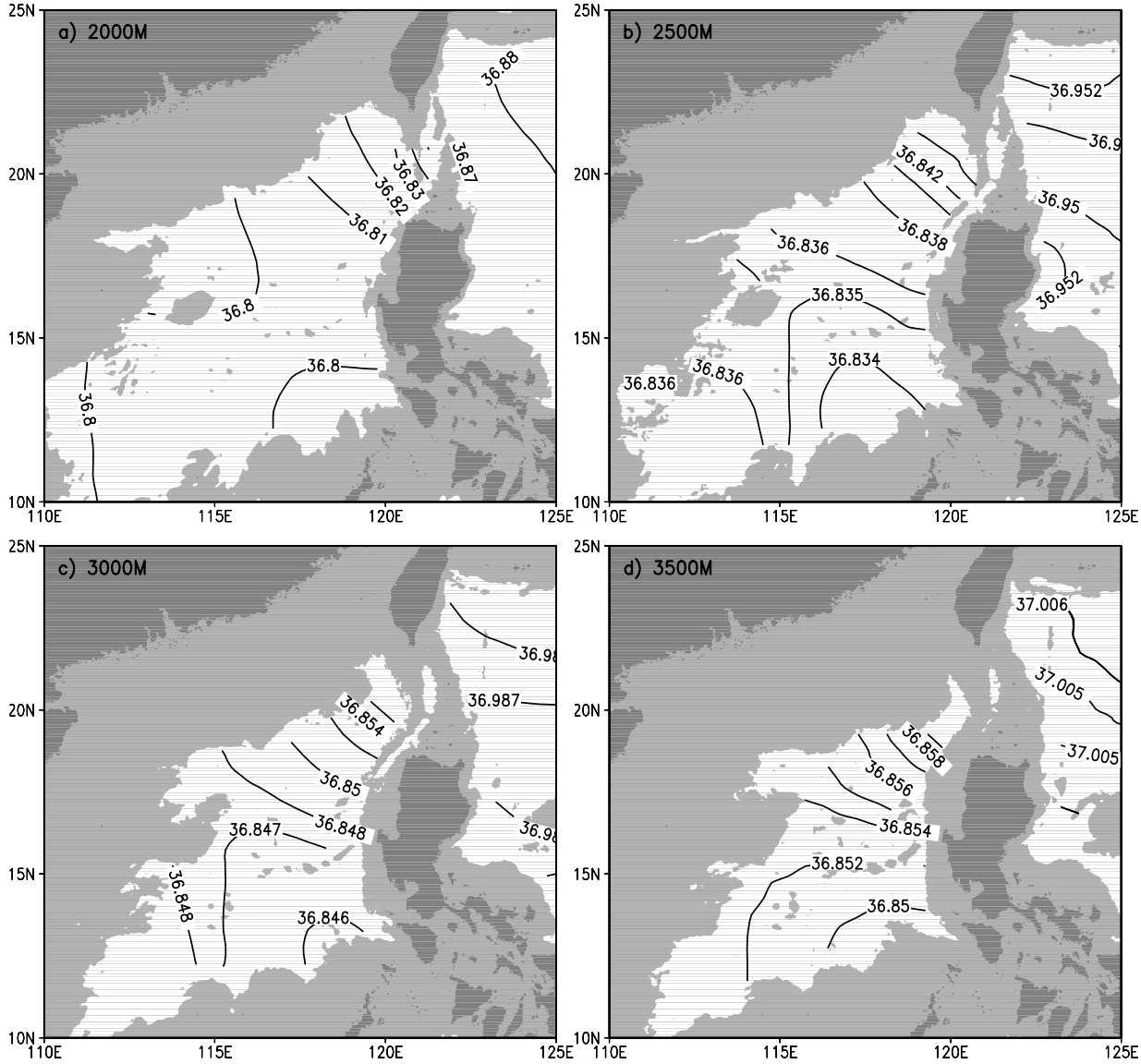

Figure 5. Potential density, σ_2, in kg m^{-3} calculated from the synthetic salinity in the deep South China Sea.

There is no easy way to quantify how much of the large salinity variations are due to errors in the data, and so it's almost impossible to clean up the data without suspicion of remaining residual bias. To get rid of the high noise level in the salinity data, we least-square fit a straight line to the adjacent Pacific data, namely, in the region (122°E–125°E, 18°N–23°N) east of the Luzon Strait (Figure 3b), and then apply this linear relation to the South China Sea potential temperature data below 1500 m to generate synthetic salinity data. Results from an analysis of these data are presented in the following sections.

4. Density Fields

[14] For the construction of horizontal maps, the temperature and newly generated salinity data from individual profiles were first linearly interpolated onto a 20-decibar uniform pressure series, and then averaged in a 0.5° × 0.5° grid regardless of the date and time of the observations. We used a variable horizontal scan-radius to include at least 10 samples at depths $\leq$3000 m and 5 samples below that depth at each grid cell, giving better resolution to the regions where data coverage is relatively good. In doing so, the scan-radius is carefully chosen to ensure that no averaging between the Pacific and the South China Sea can occur below the sill depth of the Luzon Strait. The mean property fields were smoothed using a Gaussian filter with e-folding scales of about 150 km.

[15] The density field based on the artificial salinity data in the South China Sea shows the same pattern as potential temperature field (not shown). At 2000 m, immediately above the sill depth of the Luzon Strait, potential density drops from about 36.87 kg m^{-3} on the Pacific side to about 36.84 kg m^{-3} on the South China Sea side, indicative of an inward-directed pressure gradient relative to the overlying water (Figure 5a). Elsewhere, σ_2 stays rather uniform in the

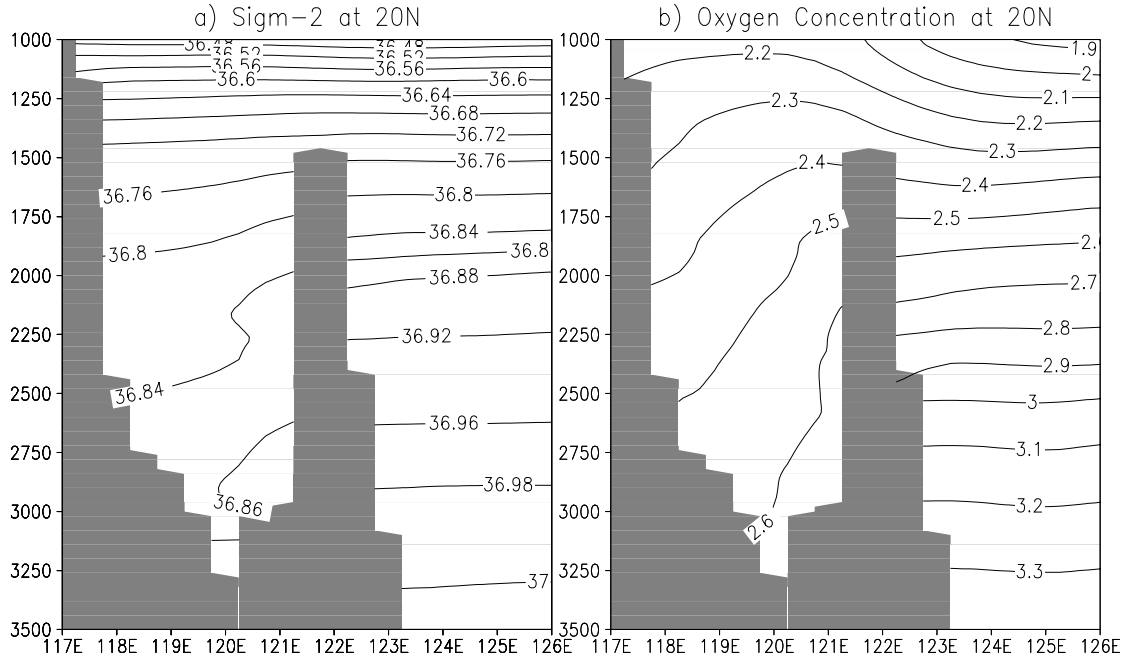

Figure 6. Potential density, σ_2, in kg m^{-3} and oxygen concentration in mL L^{-1} at 20°N. Shading corresponds to bottom topography on the 0.5° grid, and so does not indicate the deepest passages through Luzon Strait.

Pacific, lying around 36.88 kg m^{-3} to the east of Luzon Strait, and decreases slightly to about 36.80 kg m^{-3} in the central South China Sea.

[16] Below the Luzon Strait sill depth of about 2200 m the South China Sea becomes a completely isolated basin with no direct water exchange to the surrounding oceans (Figure 5b). On the Pacific side, water density is relatively high, amounting to about 36.95 kg m^{-3} near the Luzon Strait. On the South China Sea side, the density field seems to be oriented with bottom topography, with relatively low density in the southeastern part of the basin and high density along the northwestern boundary. This density distribution

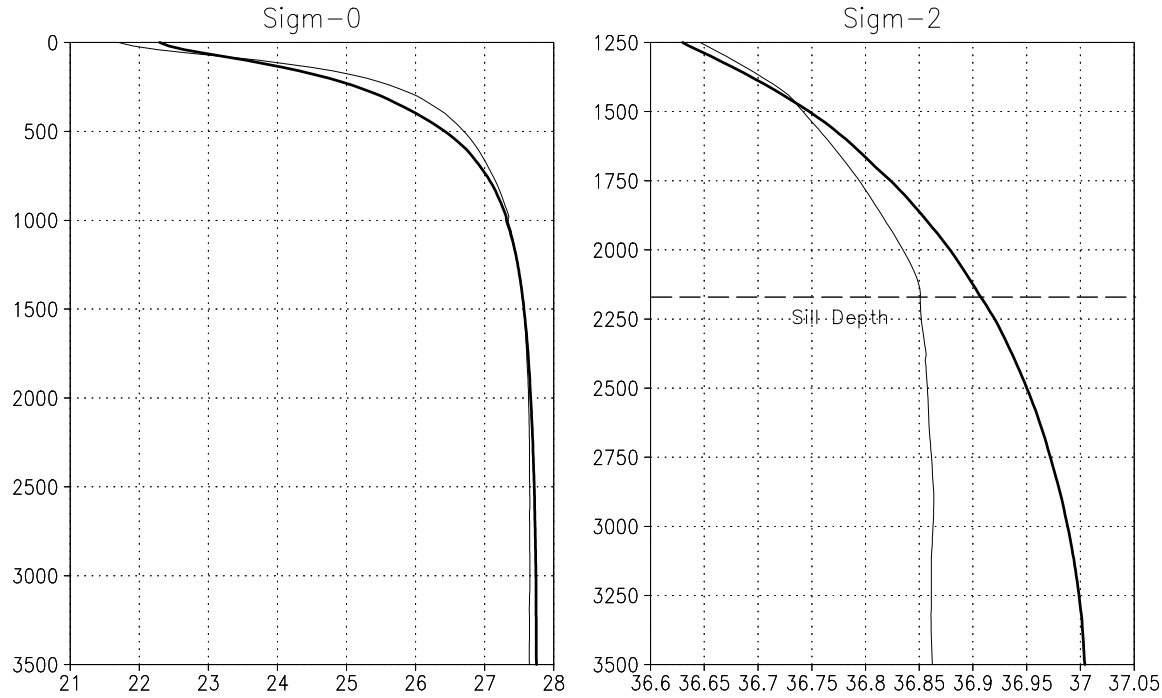

Figure 7. Vertical profiles of potential density averaged at (120°E–121°E, 19°N–21°N) on the South China Sea side (thin solid lines) and at (122°E–123°E, 21°N–23°N) on the Pacific side (thick solid lines) of the Luzon Strait. The centers of the two boxes are marked in Figure 1 as asterisks.

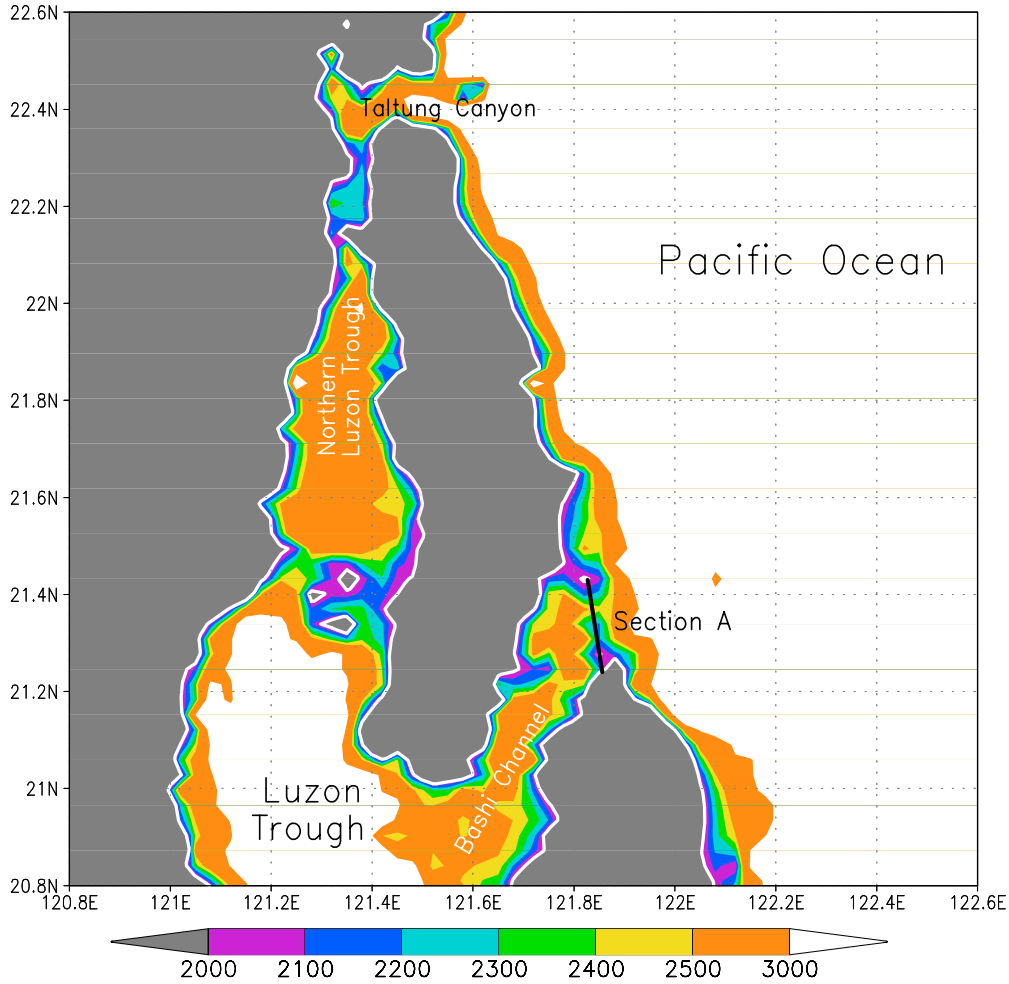

Figure 8. Bottom topography in the Luzon Strait [*Smith and Sandwell*, 1997].

could be explained as evidence of topographic steering in the South China Sea (discussed in section 6). Despite some quantitative changes, the density distribution retains almost the same pattern as we progress to the deeper layers (Figures 5c and 5d). Assuming the degrees of freedom are the same as the number of samples in each grid cell, the standard deviations can be converted to the standard errors. The typical standard errors at 3000 m, for example, are less than 10^{-3} kg m^{-3}, and reach below 6×10^{-4} kg m^{-3} in the southwestern part of the basin. The error analysis suggests that the main features shown in Figure 5 are robust.

[17] Across the Luzon Strait, there is a persistent density difference between the Pacific and the South China Sea (Figure 6). This density difference was also reported by *Qu and Lindstrom* [2004, Figure 13], though their analysis was confined only to the upper 2000 m. Here we find that water on the Pacific side is well stratified, with σ_2 increasing from about 36.48 kg m^{-3} at 1000 m to as large as 37.00 kg m^{-3} at 3500 m. No deepwater stratification is obvious on the South China Sea side, where water density is vertically uniform with a density range of only about 0.02 kg m^{-3} below 2000 m (Figure 6a). This vertical structure is consistent with oxygen distribution (Figure 6b), giving additional evidence of homogenous water properties in the deep South China Sea.

[18] A comparison of density profiles on both sides of the Luzon Strait reveals the presence of two bifurcations as defined by *Whitehead* [1998]. The first bifurcation occurs at 81 m, and the second at 1489 m (Figure 7). Water near the sea surface is of higher density in the Pacific than that in the South China Sea, reflecting strong influence of precipitation on surface salinity [e.g., *Shaw*, 1991; *Qu et al.*, 2000]. The situation is reversed at the subsurface, where intense upwelling is believed to occur in the northern South China Sea [e.g., *Chen and Wang*, 1998; *Qu*, 2002; *Yuan*, 2002]. Below 1489 m, water in the Pacific becomes denser than that in the South China Sea again, providing a baroclinic pressure gradient driving the deep overflow into the South China Sea.

5. Transport Estimate

[19] The deepwater overflow through the Luzon Strait is essentially a topographically controlled flow. The simplest estimate of its transport can be based on a reduced-gravity model, assuming conservation of potential vorticity from a deep upstream reservoir and unidirectional flow through a flat-bottomed channel (see section 2). Examination of *Smith and Sandwell*'s [1997] global bathymetric database indicates that the Luzon Strait consists of two deep channels:

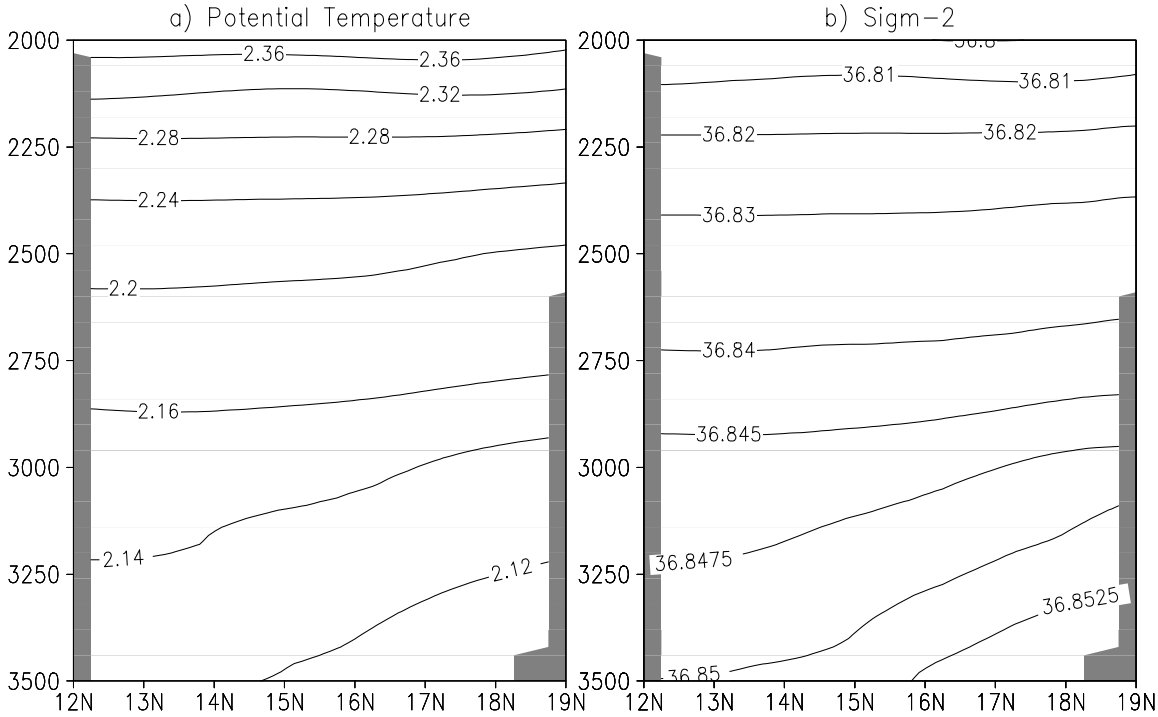

Figure 9. Potential temperature in °C and potential density, σ_2, in kg m^{-3} along 116°E.

the Taltung Canyon and the Bashi Channel (Figure 8). The Taltung Canyon is over 2500 m deep, but its connection with the Northern Luzon Trough is blocked by a shallow ridge with a sill depth of only about 2000 m. Below that depth, the only connection between the Pacific and the South China Sea is through the Bashi Channel. The shallowest sill of the Bashi Channel occurs at its eastern tip (section A), where water depth reaches 2435 only at one grid point. (Note that the horizontal resolution of the bathymetric database is approximately 4 km and that every grid point in the sill region contains at least one ship sounding.) At 2000 m, the channel along section A is about 17 km wide, and as will be seen below, is slightly wider than the Rossby radius of 16.7 km if the Coriolis parameter for 21°N is used. The depth averaged along this section is 2181 m.

[20] For purposes of estimating a volume flux, we select the depth of 2181 m as a representative depth of the channel. There is a difference in σ_2 of 5.8×10^{-2} kg m^{-3} at 2181 m (Figures 3 and 7). With the definitions given by *Whitehead* [1998], we have $g' = 5.5 \times 10^{-4}$ m s^{-2}, h_u = 692 m, and R = 16.7 km (described in section 2). Substituting these values into equation (3) gives a transport estimate of 2.5 Sv. Considering that the total volume below 1489 m in the South China Sea is 1.9×10^{15} m^3, this estimate implies a residence time of only 24 years in the deep South China Sea, well below the upper limit of 100 years given by *Broecker et al.* [1986], based on radioactive tracer measurements.

[21] This transport estimate is larger than earlier estimates by a factor of 2–3 [*Wang*, 1986; *Liu and Liu*, 1988]. As we have noted in section 1, both of these earlier studies had their limitations, and their estimates may contain large uncertainties. On the other hand, as hydraulic theory ignores complex bathymetry, overlying flow, and friction, one may have reasons to believe that this simple theory overestimates the transport. The zero potential vorticity theory has been found to overestimate mean transports by 20–50% [*Whitehead*, 1998], but errors of 100–200% would be surprising.

[22] Additional information on the deep inflow comes from dissolved oxygen data. As noted above, the South China Sea deepwater is replenished by high-oxygen water from the Pacific [see also *Qu and Lindstrom*, 2004]. Because of local biological oxygen consumption, water from the Pacific loses oxygen during its long journey toward the intermediate layer of the South China Sea. Our calculation indicates that water at its entrance of the deep South China Sea has a higher oxygen concentration (2.488 mL L^{-1}) than at its exit (2.137 mL L^{-1}), where the former is defined as the oxygen concentration averaged below 1489 m in the Luzon Strait, and the latter averaged at 1489 m over the entire South China Sea. While the rate of oxygen consumption in the deep ocean is highly uncertain, its sign is not in doubt, so at a minimum the oxygen data verify the existence of a deep inflow from the Pacific. Combining this oxygen difference with the estimated residence time from the hydraulic theory, we obtain a mean oxygen consumption rate or what is often termed oxygen utilization rate of 0.014 mL L^{-1} yr^{-1}. This value is large compared with its Pacific counterpart [*Martin et al.*, 1987]. Given the fact that the South China Sea is a tropical subbasin, where export of organic matter from the surface is large, our result is not a surprise. On the basis of a one-dimensional advection-diffusion model and synoptic observations, *Lin et al.* [1996] recently found that the oxygen utilization rate in the deep South China Sea could be as large as 0.0095 mL L^{-1} yr^{-1}, nearly as large as our estimate.

[23] Once an inflow magnitude has been determined, it becomes possible to estimate the abyssal mixing required to maintain the density contrast across the sill. We assume that the density field is steady so it must be achieved by a steady balance between inflow of water through the Luzon Strait and diapycnal upwelling of that same volume flux in the South China Sea [*Whitehead and Worthington*, 1982; *Hogg et al.*, 1982; *Roemmich et al.*, 1996]. The buoyancy gain by the upwelled water must be supplied through vertical turbulent diffusion. An estimate of the effective diffusivity required to balance the incoming buoyancy flux can be made using the formula $\kappa = \frac{Q\Delta\sigma_2}{A\partial\sigma_2/\partial z}$. In this formula $\Delta\sigma_2 = 0.06$ is the density difference between the Pacific water flowing in and water upwelling at a particular depth in the South China Sea. We have taken the value at 2000 m from the thin profile in Figure 7. We take the stratification to be $\partial\sigma_2/\partial z = 1.1 \times 10^{-4}$ kg m^{-4} from the same figure at the same depth. The area of the South China Sea at 2000 m is estimated as $A = 9 \times 10^{11}$ m^2. These numbers, along with the hydraulic estimate of volume flux into the South China Sea of $Q = 2.5 \times 10^6$ m^3 s^{-1}, produce a value of $\kappa = 1.5 \times 10^{-3}$ m^{2}s^{-1}, which is significantly larger than values commonly estimated from basin-scale abyssal mixing budgets [*Munk*, 1966; *Morris et al.*, 2001]. Uncommonly large mixing in the South China Sea is not unexpected, however, given the presence of strong internal tides propagating from Luzon Strait [*Niwa and Hibiya*, 2004; *Zhao et al.*, 2004] as well as the many regions with rough bottom topography throughout the sea (Figure 1). An estimate of the average vertical upwelling velocity of the water in the South China Sea is $w = Q/A = 2.8 \times 10^{-6}$ m s^{-1}.

[24] A similar approach involving advective-diffusive balance was taken by *Wang* [1986] to estimate the deep inflow from the scale height ($\frac{\partial\sigma_2}{\partial z} / \frac{\partial^2\sigma_2}{\partial z^2} = \frac{\kappa}{w}$) of individual density profiles. Interestingly, scale heights near the sill depth estimated from Figure 7 are 200–400 m, much less than the 1500–10,000 m reported by *Wang* [1986], so we are unable to reproduce this earlier result. The discrepancy may result from the use of individual profiles rather than a mean profile as is done here. Nevertheless, our scale heights are consistent with our mixing and transport values estimated previously.

6. Deep South China Sea Circulation

[25] Water properties in the deep South China Sea are heavily influenced by the overflow through the Luzon Strait. Upon entering the South China Sea, the dense Pacific water sinks, and as density distribution has indicated (Figure 5), tends to spread along the continental margin off southeast China. The spreading of Pacific water is particularly evident on vertical sections (Figure 9). On a meridional section at 116°E, for example, uplifted isotherms and isopycnals indicative of a bottom-intensified boundary current carrying dense Pacific water westward are seen near the northern boundary. As it spreads over the South China Sea, water from the Pacific gradually gets mixed with its surroundings, loses its Pacific characteristics, and returns in less dense layers.

[26] The property distributions described above give additional evidence of topographic steering. With the constraint of potential vorticity conservation, the dense Pacific water is expected to follow the *f*/*H* contours, which are approximately parallel to the local isobaths, *H*. Calculation of potential vorticity, $\rho^{-1}f\,\partial\rho/\partial z$, confirms this speculation (Figure 10a). Below the sill depth of the Luzon Strait, potential vorticity is much lower in the South China Sea than in the Pacific. Its contours are oriented with bottom topography, especially along the western boundary. From this distribution a deep layer circulation could be deduced. Upon entering the South China Sea through the Luzon Strait, water of Pacific origin first turns northwestward and then turns southwestward along the continental margins off southeast China and east Vietnam. This suggests that the deep-layer circulation in the South China Sea is predominantly cyclonic.

[27] The intrusion of deep Pacific water is also evident in oxygen distribution used as a passive tracer (Figure 10b). Along the continental margin off southeast China, water has an elevated oxygen level, confirming its Pacific sources. Oxygen concentration drops southeastward, approaching its minimum around the southeastern corner of the basin [*Qu*, 2002]. Another important evidence of the intrusion comes from sediment measurements. Sediment cores raised at 1500–2000 m from the continental margin off southeast China show that a significant amount of material there originates off east Taiwan, in quite a distance to the northeast of the coring sites [*Lüdmann et al.*, 2005; *Kienast et al.*, 2005]. This sediment distribution is most likely a direct consequence of deepwater overflow from the Pacific. The flow may pick up slope sediments off east Taiwan and bring them all the way into the northern South China Sea as a narrow western boundary current. In the continental margin south of China and around the Dongsha Island, in particular, the flow slows down, and part of it upwells as a result of orographic lifting, giving rise to deposition of sediments resuspended off east Taiwan. Although this deep layer circulation in the South China Sea has not yet been confirmed by direct measurements, its existence is clearly seen in high-resolution general circulation models (A. Ishida, personal communication, 2005) [see also *Qu et al.*, 2004].

7. Summary

[28] This study provides a zero-order but likely the most comprehensive description to date of water property distributions in the deep South China Sea. Most importantly, our analysis reveals that below about 1500 m there is a persistent density difference between the South China Sea and the Pacific across the Luzon Strait. This density difference is identified as a baroclinic pressure gradient driving flow from the Pacific into the South China Sea. Applying hydraulic theory with assumptions of zero potential vorticity and flat bottom to the Luzon Strait yields a transport estimate of 2.5 Sv, implying a residence time of less than 30 years in the deep South China Sea. The flux is also associated with an estimate of mean diapycnal diffusivity as large as 10^{-3} m^2 s^{-1}, and an estimate of abyssal upwelling rate of about 3×10^{-6} m s^{-1}, both of which are relatively large compared with other oceans.

[29] The transport estimate is supported by oxygen observations. Recent studies indicate that the oxygen utilization

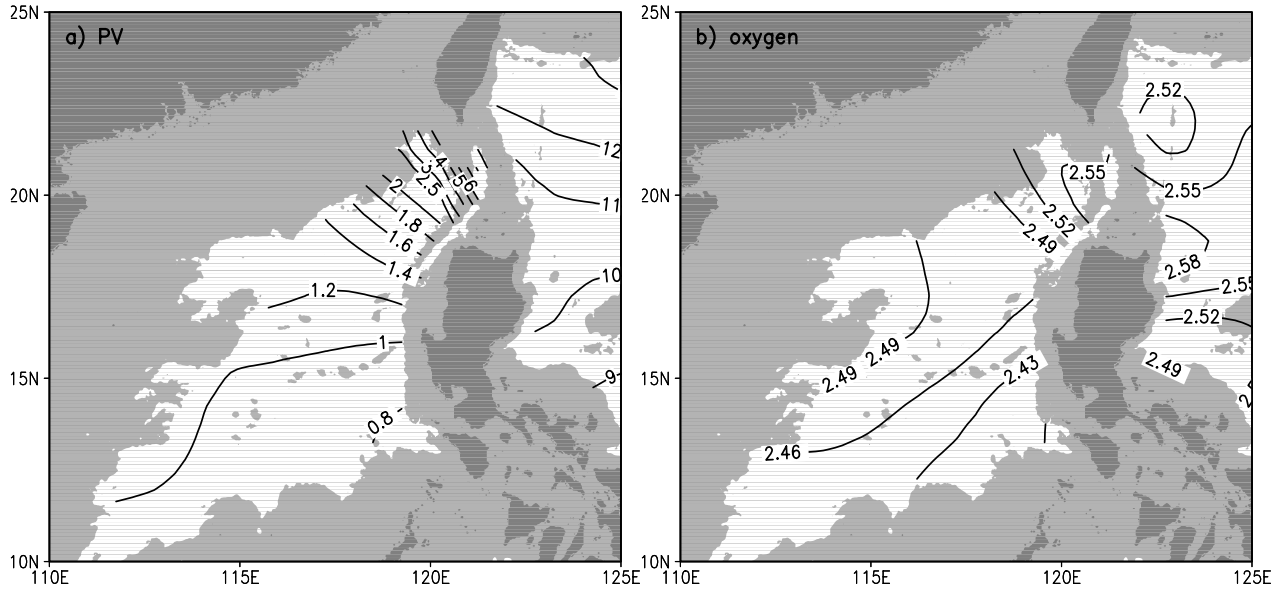

Figure 10. (a) Potential vorticity, defined as $\rho_0^{-1} f\, \partial\rho/\partial z$ (10^{-12} m^{-1} s^{-1}), and (b) dissolved oxygen concentration (mL L^{-1}) along $\sigma_2 = 36.84$ density surface, lying at depths roughly between 2000 and 3000 m in the South China Sea. Here f is the Coriolis parameter, $\partial\rho/\partial z$ is the vertical density gradient, and ρ_0 is a constant reference density (10^3 kg m^{-3}).

rate in the deep South China Sea is larger by a factor at least 3 than its Pacific counterpart. The larger oxygen utilization rate suggests a deepwater residence time of 37 years, or, equivalently, a transport of 2.0 Sv, and these values are consistent with our estimates based on hydraulic theory. Given the fact that hydraulic theory tends to overestimate mean transports of denser overflows by 20–50%, our estimates likely provide an upper bound of deepwater transport through the Luzon Strait, or equivalently a lower bound of deepwater residence time in the South China Sea.

[30] The overflow through the Luzon Strait may have a notable impact on the circulation and water property distributions in the deep South China Sea. At depths below 2000 m, water has lower potential temperature and higher potential density near the western boundary than in the central part of the basin. Upon entering the South China Sea via the deep Bashi Channel in the Luzon Strait, water from the Pacific tends to follow potential vorticity contours, approximately parallel to the local isobaths. Presently available evidence suggests a cyclonic deep boundary current system, as might be expected for an overflow-driven abyssal circulation. This current system allows Pacific characteristics to spread southwestward along the continental margin off southeast China and east Vietnam before being mixed away in the basin interior. The fact that all of the inflowing waters must warm up before leaving the basin implies that this marginal sea contributes to the water mass transformations that drive the meridional overturning circulation in the North Pacific.

[31] **Acknowledgments.** This study was supported by National Science Foundation (NSF) through grant OCE00-95906 and by Japan Marine Science and Technology Center through its sponsorship of the International Pacific Research center (IPRC). Support is also from NSF grant OCE-0325102. We are grateful to K. Richards, L. Li, and two anonymous reviewers for thoughtful comments and constructive suggestions on an earlier version of this manuscript. Thanks are also extended to Y. Du and M. Kienast for useful discussions on the topic. School of Ocean Earth Science and Technology contribution 6642 and IPRC contribution IPRC-346.

References

Broecker, W. S., W. C. Patzert, J. R. Toggweiler, and M. Stuive (1986), Hydrography, chemistry, and radioisotopes in the southeast Asian basins, *J. Geophys. Res.*, *91*, 14,345–14,354.

Chen, C.-T., and S.-L. Wang (1998), Influence of the intermediate water in the western Okinawa Trough by the outflow from the South China Sea, *J. Geophys. Res.*, *103*, 12,683–12,688.

Chu, T. Y. (1972), A study of the water exchange between Pacific Ocean and the South China Sea, *Acta Oceanogr. Taiwan.*, *2*, 11–24.

Gill, A. E. (1977), The hydraulics of rotating channel flow, *J. Fluid Mech.*, *90*, 641–671.

Hogg, N., P. Biscaye, W. Gardner, and W. J. Schmitz Jr. (1982), On the transport and modification of Antarctic Bottom Water in the Vema Channel, *J. Mar. Res.*, *40*, Suppl., 231–263.

Kienast, M., M. J. Higginson, G. Mollenhauer, T. I. Eglinton, M.-T. Chen, and S. E. Calvert (2005), On the sedimentological origin of down-core variations of bulk sedimentary nitrogen isotope ratios, *Paleoceanography*, *20*, PA2009, doi:10.1029/2004PA001081.

Lin, H., W. Han, and Y. Cai (1996), The consumption rate of dissolved oxygen in abyssal basin water of the northeastern South China Sea, *Oceanogr. China*, *6*, 103–108.

Liu, C.-T., and R.-J. Liu (1988), The deep current in the Bashi Channel, *Acta Oceanogr. Taiwan.*, *20*, 107–116.

Lüdmann, T., H. K. Wong, and K. Berglar (2005), Upward flow of North Pacific Deep Water in the northern South China Sea as deduced from the occurrence of drift sediments, *Geophys. Res. Lett.*, *32*, L05614, doi:10.1029/2004GL021967.

Martin, J. H., G. A. Knauer, D. M. Karl, and W. W. Broenkow (1987), VERTEX: Carbon cycling in the northeast Pacific, *Deep Sea Res., Part A*, *34*, 267–285.

Morris, M. Y., M. M. Hall, L. C. St. Laurent, and N. G. Hogg (2001), Abyssal mixing in the Brazil Basin, *J. Phys. Oceanogr.*, *31*, 3331–3348.

Munk, W. (1966), Abyssal recipes, *Deep Sea Res.*, *13*, 707–730.

Nitani, H. (1972), Beginning of the Kuroshio, in *Kuroshio: Physical Aspects of the Japan Current*, edited by H. Stommel and K. Yoshida , pp. 129–163, Univ. of Wash. Press, Seattle.

Niwa, Y., and T. Hibiya (2004), Three-dimensional numerical simulation of M2 internal tides in the East China Sea, *J. Geophys. Res.*, *109*, C04027, doi:10.1029/2003JC001923.

Qu, T. (2002), Evidence of water exchange between the South China Sea and the Pacific through the Luzon Strait, *Acta Oceanol. Sin.*, *21*, 175–185.

Qu, T., and E. Lindstrom (2004), Northward intrusion of Antarctic Intermediate Water in the western North Pacific, *J. Phys. Oceanogr.*, *34*, 2104–2118.

Qu, T., H. Mitsudera, and T. Yamagata (2000), Intrusion of the North Pacific waters into the South China Sea, *J. Geophys. Res.*, *105*, 6415–6424.

Qu, T., Y. Y. Kim, M. Yaremchuk, T. Tozuka, A. Ishida, and T. Yamagata (2004), Can Luzon Strait transport play a role in conveying the impact of ENSO to the South China Sea?, *J. Clim.*, *17*, 3643–3656.

Roemmich, D., S. Hautala, and D. Rudnick (1996), Northward abyssal transport through the Samoan passage and adjacent regions, *J. Geophys. Res.*, *101*, 14,039–14,055.

Shaw, P.-T. (1991), Seasonal variation of the intrusion of the Philippine sea water into the South China Sea, *J. Geophys. Res.*, *96*, 821–827.

Smith, W. H. F., and D. T. Sandwell (1997), Global sea floor topography from satellite altimetry and ship depth soundings, *Science*, *277*(5334), 1956–1962.

Wang, J. (1986), Observation of abyssal flows in the Northern South China Sea, *Acta Oceanogr. Taiwan.*, *16*, 36–45.

Whitehead, J. A. (1989), Internal hydraulic control in rotating fluids—Applications to oceans, *Geophys. Astrophys. Fluid Dyn.*, *48*, 169–192.

Whitehead, J. A. (1998), Topographic control of oceanic flows in deep passages and straits, *Rev. Geophys.*, *36*, 423–440.

Whitehead, J. A. (2003), Constant potential vorticity hydraulically controlled flow-complexities from passage shape, *J. Phys. Oceanogr.*, *33*, 305–312.

Whitehead, J. A., and L. V. Worthington (1982), The flux and mixing rates of Antarctic Bottom Water within the North Atlantic, *J. Geophys. Res.*, *87*, 7903–7924.

Whitehead, J. A., A. Leetmaa, and R. A. Knox (1974), Rotating hydraulics of strait and sill flows, *Geophys. Fluid Dyn.*, *6*, 101–125.

Wyrtki, K. (1961), Physical oceanography of the southeast Asian waters, *Naga Rep. 2*, 195 pp., Scripps Inst. of Oceanogr., La Jolla, Calif.

Yuan, D. (2002), A numerical study of the South China Sea deep circulation and its relation to the Luzon Strait transport, *Acta Oceanol. Sin.*, *21*, 187–202.

Zhao, Z. X., V. Klemas, Q. N. Zheng, and X. H. Yan (2004), Remote sensing evidence for baroclinic tide origin of internal solitary waves in the northeastern South China Sea, *Geophys. Res. Lett.*, *31*, L06302, doi:10.1029/2003GL019077.

J. B. Girton, Applied Physics Laboratory, University of Washington, 1013 NE 40th Street, Seattle, WA 98105-6698, USA. (girton@apl.washington.edu)

T. Qu, International Pacific Research Center, SOEST, University of Hawaii, 2525 Correa Road, Honolulu, Hawaii 96822, USA. (tangdong@hawaii.edu)

J. A. Whitehead, Department of Physical Oceanography, Woods Hole Oceanographic Institution, MS 21, Woods Hole, MA 02543-1541, USA. (jwhitehead@whoi.edu)